INTEGRATING OPTICAL AND RADAR IMAGERY TO ENHANCE RIVER DROUGHT MONITORING

S. Conversi [1] *, D. Carrion [1], A. Norcini [2], M. Riva [1]

[1] Dipartimento di Ingegneria Civile e Ambientale, Politecnico di Milano, Piazza Leonardo Da Vinci 32, 20133 Milano, Italy - (stefano.conversi, daniela.carrion, monica.riva)@polimi.it
[2] Struttura Natura e Biodiversità, Direzione Generale Territorio e Sistemi Verdi, Regione Lombardia, Piazza Città di Lombardia 1, 20124 Milano, Italy – alessandra_norcini@regione.lombardia.it

KEY WORDS: Remote Sensing, SAR, Spectral indices, SWM, Sensor data fusion, Drought monitoring, Biodiversity hazard

ABSTRACT:

Drought events are growingly affecting European and Italian territories, hampering local environments and biodiversity, such as the ones relying on rivers for their subsistence. Monitoring of rivers is becoming an important issue to face drought crisis and may be exploited with different tools. Among the most commons, satellite imagery is exploited to map water coverage, basing on optical or radar sources. This work proposes a combination of the two sensors to overcome possible limitations of the single dataset exploitation, reaching a reliable result. The methodology is applied to a stretch of Po River in Lombardy region (Italy). Through Google Earth Engine platform, optical satellite Sentinel-2 and radar satellite Sentinel-1 data are processed. The combination of the radar data and of the optical spectral indices is carried out through a pixel-based supervised classification, with a Random Forest classifier. Maps of water coverage are obtained, numerical outcomes of water surface evaluation are recorded and validated by the mean of reference hydrometric data. A multitemporal analysis is then reported, aiming to prove the efficiency of the procedure. All iterations show reliable accuracies and correlation among water surface estimation and water table measurements in two sections of interest. In perspective, the proposed methodology will be implemented in tools for supporting drought monitoring to be integrated in environmental public administration policies.

1. INTRODUCTION

1.1 Drought in Northern Italy

In 2022, Italy suffered one of the most severe drought periods of the last century (Levantesi, 2022), with relevant implications on biodiversity and, more in general, environmental hazards.
Several reservoirs and rivers were severely affected, among which Po River (the Italian longest water stream); direct impacts of the drought were recorded on the whole set of activities that rely on the river for their deployment, first of all the agricultural ones. In June 2022, Coldiretti estimated that the dry conditions of the major lakes and rivers resulted in at least 1/3 decrement of national agricultural production (Coldiretti, 2022). Furthermore, local water authorities were obliged to impose navigation restrictions (AIPo, 2022), resulting in evident losses for the connected sectors, such as tourism, and the Head of Italian Civil Protection Department reported as “concrete” the possibility of rationing of drinking-water (D’Amato, 2022). For the sake of completeness, it should be reminded that this extreme measure was not undertaken, nevertheless the situation remained critical for several months. The drought of 2022 caused issues also to artificial reservoirs, forcing competent bodies (such as Regione Lombardia administration) to reduce water discharges, even affecting hydropower plants systems. As a response, monitoring campaigns were promoted, aiming at preventing and potentially mitigating the effects of water scarcity (Regione Lombardia, DGR April 13th 2022, n. XI/6283).
Another crucial topic is the impact that a so dry period could have on ecosystems of the involved regions. The conditions of environmental stress may indeed have a great influence on several species’ lifecycle, possibly resulting in a severe depletion of biodiversity (Levantesi, 2022).
Global Drought Observatory (GDO) depicted in its report a particularly critical situation for Po River, due to the relevant precipitation deficit that affected its principal tributaries since 2021 winter (Toreti et al., 2022). The scarcity of rainfall was indeed a generalized problem which involved most of Southern Europe, while in Italy the most severe conditions were faced by Piedmont and Lombardy regions. The roots of such a phenomenon can be found in the concurrence of several factors: the mentioned rainfall anomaly, combined with climate conditions causing warm temperatures and consequentially poor snow accumulation in southern Alps during winter (Toreti et al., 2022). Therefore, the supply of water from snow melting was drastically reduced during spring, a condition that combined with a consistent lack of summer rainfalls, resulted in the depicted exceptional drought (Bonaldo et al., 2022). Figure 1 shows March 2022 map of European Drought Observatory’s Combined Drought Indicator, which summarizes indices on precipitations, soil moisture and vegetation stress (Toreti et al., 2022). It is evident that the affected area embeds Po River basin and that conditions resulted to be moderately severe even in early spring.

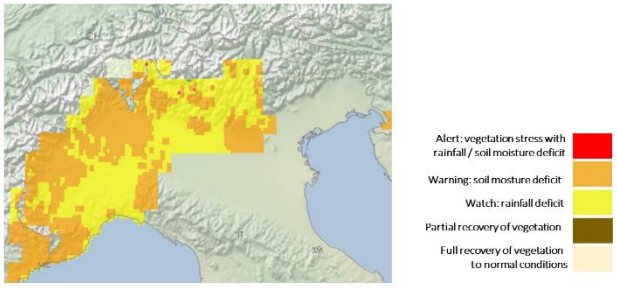

Figure 1. JRC March 2022 Combined Drought indicator map for Northern Italy, from (Toreti et al., 2022).

* Corresponding author

The drought event of 2022 is probably representing an exceptional outcome of negative climatological factor combinations, nevertheless it is experts' common opinion that the frequency of similar events may increase in the future (Bonaldo et al., 2022). Considering the vulnerability and the strategical importance of the involved areas for Italian economy and environment, it will then be necessary for public administrations to equip with tools capable of monitoring and mitigating the outcomes of such emergencies. Stated this necessity, this paper aims to provide Regione Lombardia with a tool for assessing water coverage of large rivers, exploiting remotely sensed data. Such a tool may then be used for monitoring river conditions, even during extreme events; furthermore, it will represent a support for defining drought early warning procedures and more in general policies on river management.

1.2 Remote Sensing and sensor integration for supporting land monitoring

In this work, drought monitoring goal is pursued through an integration between radar and optical satellite imagery. The final objective of the work is to give an estimation of the water extent in water bodies, in particular permanent medium-width rivers, within the monitored area. Water surface variation in water bodies, in this framework, is intended as a measure of drought conditions of river surroundings. In this sense, providing up-to-date assessment of water surface may result in a particularly useful information for decision makers (Regione Lombardia, in the study case). Such information can trigger direct actions in case they reveal the occurrence of critical environmental threats or can be used as a support for structuring in the most suitable way drought monitoring and correlated biodiversity policies. Indeed, it can be highlighted that a sudden change of water presence (both an increment or a decrement), as well as a prolonged abnormal water scarcity, can drastically hamper biodiversity, especially at a local scale.

Satellite based Remote Sensing provides optimal data for detecting water surface, both employing optical and radar imagery, as it will be discussed in paragraph 1.3. In this work, a combination of the two sensors is proposed for enhancing the quality of results and the applicability to different meteorological conditions. As an outcome of the integration, a pixel classification procedure, having as output a mask of the water surface detected in a given stretch of a river is performed.

The concept of combining different typologies of data (or sensors) takes the name of data fusion; Schmitt & Zhu (2016) provide an accurate overview of the state of the art and of the different definitions of this technique depending on procedures and field of study. Dealing with Remote Sensing, the most suitable definition for the current work is the one of *sensor data fusion*, from Gustaffson (2012): "Sensor fusion is the combining of sensory data or data derived from disparate sources such that the resulting information is in some sense better than what would be possible when these sources were used individually". Following this statement within the work it will be shown that combining the information of optical and radar sensors consents to compensate weak points of the single systems and as a result limit the overall errors. Several cases of fruitful applications of optical and radar integration can be retrieved in literature, as discussed in the following. Sensor data fusion has been exploited for automatic land cover mapping (De Fioravante et al., 2021), crops classification and mapping (Tuvdendorj et al., 2022 – Felegari et al., 2021 – Chakhar et al., 2021), as well as for monitoring growth stage of specific cultures, such as rice for Ramadhani et al. (2020).

Getting closer to water mapping, it is relevant to mention one of the most widespread applications of Remote Sensing for emergency management (especially regarding SAR imagery), which is flood and post-flood mapping, as detailed in (Carreño & De Mata, 2019) and (Li et al., 2022); nonetheless, optical imagery as well can be exploited for delineating flooded areas, as shown by (Ajmar et al., 2017), and it can also be fruitfully used in combination with different data sources, as proven by Valvassori et al. (2022), who integrated it within a Volunteered Geographic Information framework.

Most of the cited studies converge on the findings of an increment of mapping accuracy that comes when optical and radar platforms are used in combination. Finally, it is worth mentioning that also river monitoring is gradually being addressed with the support of Remote Sensing observations, also for reconstructing their dynamics and evolution (Langat et al., 2018). In this case, the proficiency of sensors integration is foreseen, as well as the necessity to increment automatization of monitoring procedures (Tomsett & Leyland, 2019), both of which are key elements of the work presented in this paper.

1.3 Satellite data and thresholding methods for water mapping

Synthetic Aperture Radar (SAR) imagery is particularly suitable for this work's purposes in terms of water detection and mapping; in fact, inland waters, due to their "smooth" surface (in case of waves absence) react as an almost perfect specular surface. This means that the signal is reflected in a different direction with respect to the sensor one. Consequently, the values of backscatter recorded by the satellite are so low that can be, in most cases, easily distinguished from whatever other surface, both in terms of values and in visualization, where water pixels appear to be much darker than the rest of landcovers (Carreño & De Mata, 2019). Furthermore, it is to be noted that radar inputs are widely used in flood detection also because the signal, in most cases, is not prone to interferences due to weather conditions such as clouds presence. The latter, as well known, is a circumstance that hampers the analysis of optical imagery (due to loss of information). Complementing radar and optical data in water surface mapping will result in a benefit for mitigating typical errors rising from both data sources.

The group of methods commonly employed for detecting water from radar imagery is the thresholding one. The main concept laying behind these methods is the possibility of deeming a pixel as belonging to a certain class on the base of its response value to SAR radiation (Landuyt et al., 2019). In operational terms, all the pixels that look dark (whose value is lower than a given threshold) are classified as water; clearly the consistency of this classification entirely rely on the capability of setting the best fitting threshold value for the case study (Bazi et al., 2005).

There exist several kinds of thresholding methods, some are just related to a binary classification (e.g. flooded/non flooded), basing the thresholding on purely statistical observations, while some others consider different classes and integrate site-related characteristics to establish the thresholds. Among these, tiled thresholding methods appear to be particularly robust, as they are characterized by the application on representative areas, whose response is carefully investigated (Landuyt et al., 2019). Histograms of response values are then plotted and the thresholds are set depending on the frequency distribution of the features of interest (Cao et al., 2019).

As anticipated, it is crucial to state that the thresholding approach in SAR image processing, although quite reliable, is still prone to errors. In particular, addressing the reference case of water detection, conditions of the ground may interfere with the response and so lead to pixel misclassification. As an example, the presence of wind may create roughness on water surfaces, thus modifying the backscattered signal direction, or there may

be double bounce or volume scattering errors in case of flooded object presence (Landuyt et al., 2019). Often, selecting the most appropriate band for the analysis depending on the in-situ conditions may help in mitigating the errors; in fact, VV stresses double bounce effects and shows a higher sensitivity to water roughening, while VH is mainly influenced by volume scattering (Twele et al., 2016). Furthermore, particular attention should be devoted to the possibility of overestimation due to the presence of waterlike surfaces (having analogous behaviour in terms of signal reflection). Presence of shadows will give "darker" pixels and, finally, background noise can create diffused errors on the area of study, as in the case of responses impaired by high levels of soil humidity (Carreño & De Mata, 2019).
As a last remark, multispectral indices computed from optical satellite images can be exploited with thresholding approaches as well; in this case, thresholding is applied to the values of the indices themselves. In this work, both radar and optical thresholding methods are considered as reference solutions to evaluate the quality of the results of classification obtained by integrating Sentinel-1 and Sentinel-2 data.

2. METHODOLOGY

2.1 Dataset pre-processing and reference maps

In this paragraph the methodology proposed for mapping water through the integration of optical and radar data is described. It is to be remarked that it is specified for datasets from European Space Agency's Sentinel-1 (S-1) and 2 (S-2) constellations, but it can be generalized for whichever optical and radar combination capable of sampling information on the same bands.
Images collected from the two sensors are pre-processed and exploited to obtain reference water coverage maps, by the mean of thresholding methods. Subsequently, the datasets combination is performed through a classifier, whose outcome is a new water coverage map taking both radar and optical images as inputs; the complete workflow is depicted in Figure 2 and detailed below. The procedure is implemented in Google Earth Engine environment, and satellite imagery is reached through its *Data Catalog*, containing, among the others, the collection of Sentinel-1 and Sentinel-2 datasets (GEE, 2023).

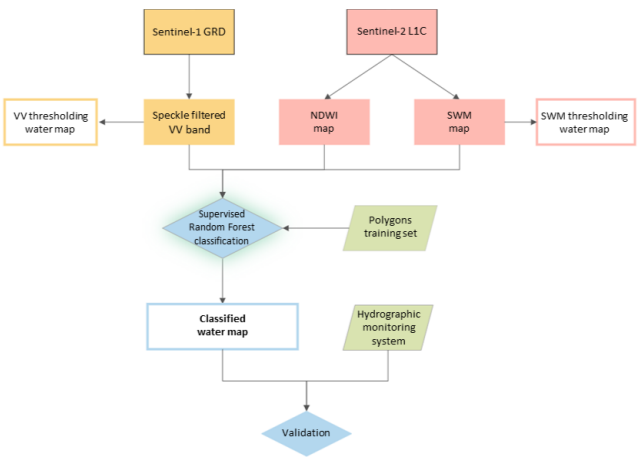

Figure 2. Workflow of water coverage maps production integrating Sentinel-1 and Sentinel-2.

The GEE platform, used for implementing the methodology, can be defined as a cloud-based Google service for planetary geospatial analysis (Gorelick et al., 2017). It consents to develop scripts in JavaScript language employing both uploaded datasets and imagery available in its own catalogue. The code is run in the same environment, the processing is carried out on Google servers and then outcomes are displayed locally. This tool allows the computation of large sets of images to support multitemporal assessment on wide areas without the need of downloading locally any kind of data and taking advantage of powerful cloud computing. Nevertheless, results can be exported and then investigated and processed also in Desktop GIS.
To cover the area of interest, a mosaicking of images, both for S-2 and S-1, has been performed, with the approximation of including different tiles acquired in different dates. Clearly a date range is defined, to ensure that these tiles combination are significative. In this regard, a function for selecting the smaller possible temporal interval is built, so to select from the collection images as close as possible in time, to guarantee, at the same time, at least 90% of study area spatial coverage and a maximum of 20% cloud presence (in S-2 case).
For Sentinel-1 data retrieval the procedure is analogous, but it is to be considered that the orbits of the two constellations are not identical, meaning that the total coverage of the area for both sensors can differ. In this case, a procedure to define the time range for S-1 acquisition as close as possible to S-2 ones is developed. In addition, S-1 product (L1C, band VV) is subjected to a procedure of filter speckling, so to obtain a radiometric corrected image in which granular noise is removed, obtaining a more suitable base for the following procedures (Carreño & De Mata, 2019).
Aiming to compare the results of the thematic maps that are produced as outcome of the whole procedure, a couple of water mask maps obtained with a classic thresholding approach are built. Regarding SAR case, an analysis of values with photointerpretation is performed and the value of -18 dB is considered as threshold, in agreement with commonly used values of backscatter intensity, which is set around -20 dB (Carreño & De Mata, 2019).
The second water map that is produced is based on Sentinel-2, where the thresholding is applied to a specific band combination named Sentinel Water Mask (SWM, Milczarek et al., 2017). The developers of SWM suggest as an optimal range of values for water detection 1.4-1.6 and, after visual interpretation, the procedure is deployed with a 1.4 threshold. Another S-2 bands combination is applied for obtaining a different spectral index, the Normalized Difference Water Index (NDWI), which was developed to monitor the response of water content in vegetation leaves (JRC, 2011). In optimal conditions it provides a univocal response in case of pixels associated to water surfaces, so it is involved in the process of S-1 and S-2 integration. The formulation of the mentioned two indices is available in (1) and (2).

$$SWM = \frac{(B2+B3)}{(B8+B11)} \quad (1)$$

$$NDWI = \frac{(B3-B8)}{(B3+B8)} \quad (2)$$

where B2 = blue band TOA reflectance, B3 = green band TOA reflectance, B8 = near-infrared TOA reflectance, B11 = first shortwave infrared band reflectance.

2.2 Optical and radar sensors integration for water detection

The integration between the two sensors is obtained exploiting a supervised machine learning classification algorithm,

considering as an input both the data sources. A Random Forest classifier with 10 decision trees (Breiman, 2001) is chosen. This kind of approach results to be particularly suitable for the case study, because its structure consents to improve, with respect to other algorithms, the classification of pixels with unknown distribution and frequency (De Fioravante et al., 2021).
To train the supervised algorithm, a set of polygons deemed as representative of the two classes of interest for the study (water and non-water) is selected. A different set of polygons is created by photointerpretation of RGB imagery. The selected polygons are then randomly split, 20% as training set and 80% as test sample. The classification itself takes as input the bands of filtered VV for Sentinel-1 and the indices SWM and NDWI for Sentinel-2. The outcome of the procedure is then a thematic map containing two different classes of pixels, associated to water and non-water. Aiming to have a parameter for quantifying the results and perform comparison among epochs, the area of water pixels is calculated, within a buffer of 600 m from the river vector, so that the solution will not take into account possible misclassified pixels or secondary water surfaces not belonging to the river.
Validation is later performed with a set of 5000 randomly extracted points (independent from the ones contained in training and test polygons), in order to estimate the amount of correctly classified pixels, false positives and false negatives. As a measure of classification accuracy, the True Positive Ratio (TPR) is used, which takes into account the ratio between the number of pixels that are correctly classified against the total number of positives (Ting, 2011), in this case, of pixels corresponding to water. The same parameter is calculated also for the reference thematic maps obtained with VV and SWM thresholding, so to have a comparison on the quality of results for the proposed method. In addition, the outcomes are also matched with the reference data coming from hydrological stations installed along the river. The reference parameter considered is the mean hydrometric level calculated on the interval of time on which the mosaicked images are built. This further dataset integration consents to verify the consistency of the approach in terms of variation of water quantity in the stream and, in a multi-temporal point of view, to monitor the evolution of the river surface.

3. STUDY AREA AND REFERENCE DATA

The datasets considered in this work as radar and optical input are respectively Sentinel-1 and Sentinel-2 imagery. The ground resolution of 10 m, available for the considered products of both satellites, allows to detect variations in river surface during a drought period and the revisit times (5 days for S-2, 6 days for S-1) consent to have a sufficiently dense series of imagery exploitable for monitoring purposes (ESA, 2023a; 2023b). Furthermore, these datasets are reachable for free, a crucial condition in perspective of the application of the work in public administration procedures. Images are made available by Copernicus Open Access Hub (Gascon et al., 2017) and, for the interest of the present work, retrieved through Google Earth Engine (GEE) platform. Top-Of-Atmosphere (Level 1-C scenes) reflectance images are used for the 13 sampled bands of Sentinel-2, while for Sentinel-1 Level-1 Ground Range detected (GRD) product is considered. Among the available radar bands, the single co-polarization Vertical transmit/Vertical receive (VV) is selected for the study.
Reference data regarding the hydrometric records along Po River are reached from the monitoring network of the Interregional Agency for the Po River (AIPo), which is a public entity providing engineering and environmental services to the bodies involved in Po River management (AIPo, 2023a). This organization acquires and shares data coming from a network of 84 hydrological stations distributed along the river, each of which is associated with a fluvial section. Provided datasets contain, apart from physical description of the sections themselves, historical records of the water table level available at different frequencies, up to 5 minutes measurements, with centimetric precision.
Through the years, several campaigns for increasing the density of monitoring network were carried out, enlarging the number of instrumented sections, thus providing an ever-growing detail on water level distribution along the river. For the current work the most updated subdivision is considered, which dates back to 2005, reachable through AIPo geodata portal (AIPo, 2023b).
As study case, a representative portion of Po River delimited by two subsequent monitored sections has been selected, aiming to outline an area embedding diverse peculiarities in river morphology, such as presence of multiple bends and small lenses of emerging ground within the stream itself.
Hydrometric datasets and reports of competent authorities on hydrological monitoring on Po River were considered and the portion of river flowing from Spessa Po (section code S7D) to Piacenza (S20) was then considered. Stated the representativity of this portion of the river, it is interesting to highlight that the two considered sections result to be among the most impaired by 2022 drought event (Autorità di Bacino Distrettuale del Fiume Po, 2022). Aiming to provide some evidences, Spessa Po showed a huge decrement in several indicators, among which the monthly mean flow rate, that went from the reference value of 1100 m^3/s to 265 m^3/s, according to October 2022 bulletin (Autorità di Bacino Distrettuale del Fiume Po, 2022). This so relevant variation is also supported by the official indicators mentioned in the introduction, the ones provided by Global Drought Observatory of the Copernicus Emergency Management Service (GDO, 2023). In Figure 3, the trend of Standardized Flow Index for the section of Piacenza in the period October 2021-September 2022 is depicted, clearly confirming the extreme hydrological drought in the considered area (Toreti et al., 2022).

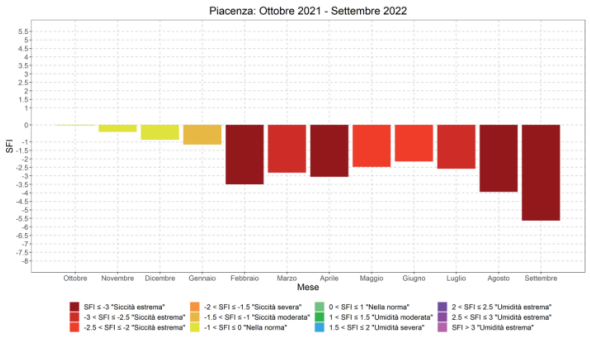

Figure 3. Standardized Flow Index calculated in Piacenza section (October 2021 – September 2022), from (Autorità di Bacino Distrettuale del Fiume Po, 2022).

4. RESULTS

In this paragraph the outcomes of the applied methodology are shown, with respect to a sample time span taken as a reference: from 21st to 31st of May 2022. Water coverage maps coming from the single SAR and NDWI thresholding will be presented, as well as the one resulting from integrated Sentinel-1 and Sentinel-2 classification. Furthermore, some considerations regarding the correspondence with hydrometric records will be expressed, along with a summary of results for the whole set of dates considered in this work.

As it can be seen in Figure 4, the analysed river portion is clearly delineated and represented by the light blue pixels, which have been classified as water; in the background the corresponding RGB Sentinel-2 mosaic is displayed. The water surface estimation for this computation is 13.48 km^2.

Figure 4. Water coverage map of the entire study area obtained integrating S-1 and S-2 data for the reference period 21st-31st May 2022.

Figures 5a and 5b represent the two boundary sections of the portion of interest of the river, with the continuous blue line standing for the mean water heights (above the sea level) evaluated for the time window considered for imagery retrieval: 56.05 m in Spessa Po and 54.52 m in Piacenza. The red dashed line represents the hydrometric zero, which corresponds to the reference water height value for the instrument installed in each of the sections. Matching these two observations, delta of -1.95 m and -0.48 m are retrieved, respectively for Spessa Po and Piacenza. Aiming to draw a comparison with previous years, the delta evaluated for the same date interval in Spessa Po amounted to -0.27 m in 2020 and -1.39 m in 2021, while for Piacenza they resulted in +1.26 m in 2020 and +0.13 m in 2021. This numerical assessment already gives a clear idea of the scarcity of water in the reference period, as supported by the official bulletins of the local agency (Agenzia Distrettuale per il Bacino del Po, 2022).

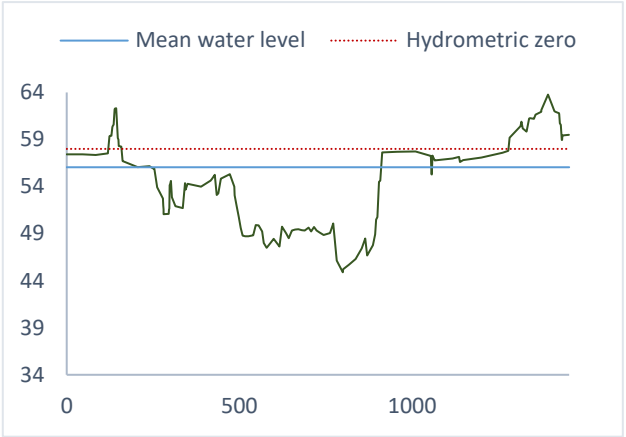

(a)

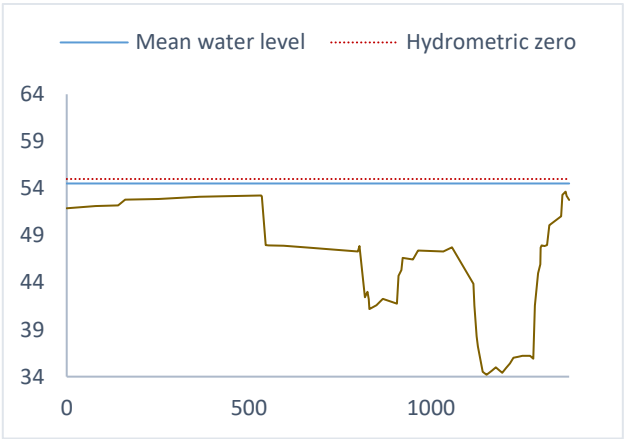

(b)

Figure 5. Mean hydrometric level recorded by AIPo stations in the reference period 21st-31st May 2022 for the sections of Spessa Po (a) and Piacenza (b).

It is worth noting that for the considered interval of dates the mosaicked S-2 imagery shows the presence of a partial cloud coverage. In fact, it is an interesting situation to prove the potential of the satellite imageries integration. As depicted in Figure 6a, SWM thresholding approach is lacking information, due to the physical obstacle that clouds represent for the optical sensor. On the other hand, radar signal appears to be unclear too, leading to a diffuse misclassification and overestimation of water pixels (Figure 6b), which can presumably be due to noise in the signal. Comparing Total Positive Ratio values for the three classifications these comments are corroborated. Indeed, the TPR for SAR thresholding amounts to 69.1%, it is increased in SWM-derived map up to 82.7%, while for the integrated classification reaches the value of 90.2%. The solution proposed in this work represents the best performing process, in terms of accuracy,

among the ones considered, thus proving the capacity of the proposed integrated approach to overcome the main issues that arise from each single sensor. Obviously, this result depends on the accurate and time-related selection of training polygons, so to consider the different possible misclassifications and adequately train the machine learning algorithm.

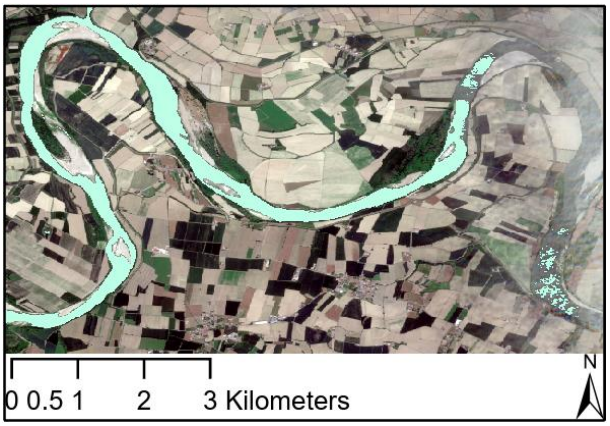

(a)

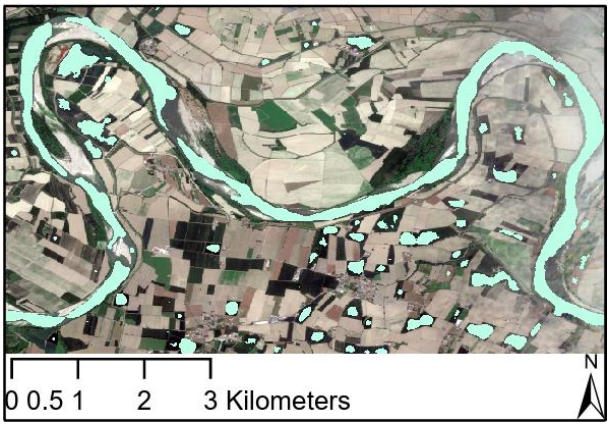

(b)

Figure 6. Detail of water coverage maps for the reference period obtained by thresholding (a) optical imagery - SWM index and (b) radar imagery - VV filtered band. Errors can be recognized in both: (a) shows loss of data due to cloud presence, while in (b) overestimation of water in terrains surrounding the river can be noted.

As mentioned, the proposed analysis is repeated for a set of different dates. Aiming to ensure a comparability among the results, it was decided to carry out the calculations for a couple of significant periods in each year, corresponding to the average positive and negative peaks of water level. So, late spring (May/June) and late summer (August) computations are performed, from 2016 to 2022. The year 2023 is then addressed with a different set of dates, with the aim of investigating the possible ongoing consequences of the drought event witnessed in 2022; furthermore, the system is also tested for the monitoring of multiple flood events that affected the area in May 2023 (Povoledo, 2023).
Table 1 contains all outcome values and accuracies obtained with the application of the proposed methodology on the whole period of interest. It is to be highlighted that for all computations, the TPR obtained with the integrated approach is higher than 85%. In addition, the trend of the estimated water surfaces results to be coherent with both hydrometric levels and known meteorological events that involved the area, as discussed in the following. The lowest value of water surface is found in August 2022 (during the severe drought), amounting to 12.53 km^2. The highest value is retrieved in concomitance with the May 2023 flood (evaluations referred to imagery taken immediately after the event) with an estimated area of 19.25 km^2, against a mean value for the late Spring in previous years of 15.95 km^2 and 13.46 km^2 in the former assessment of February 2023.

Period	Water surface [km^2]	TPR [%]	Level Spessa Po [m]	Level Piacenza [m]
2016 May	16.05	87.9	57.295	55.005
2016 Aug	13.59	85.5	56.207	55.001
2017 May	14.51	88.2	56.804	55.270
2017 Aug	14.36	85.5	56.215	54.652
2018 Jun	18.58	90.8	57.872	56.548
2018 Aug	14.79	90.5	56.326	54.826
2019 Jun	15.47	86.7	57.143	55.611
2019 Aug	16.14	93.3	56.643	55.063
2020 May	17.73	89.3	57.943	56.511
2020 Aug	14.83	91.3	57.166	54.737
2021 May	15.83	91.0	56.513	55.040
2021 Aug	15.02	96.2	56.299	54.877
2022 May	**13.48**	**90.2**	**56.051**	**54.522**
2022 Aug	12.53	86.4	55.697	54.246
2023 Feb	13.16	90.5	55.884	54.555
2023 May	13.43	91.3	56.137	54.644
2023 May	19.25	96.8	57.982	56.596

Table 1. Collection of results of the methodology application for the whole set of dates (2016 – 2023). The line in bold refers to the sample case detailed in Paragraph 4. May 2023 presents two records, respectively pre and post multiple floods event.

Finally, it was interest of the authors to explore the correlation between the levels of water table measured by hydrometrical network and the estimated water surfaces, considering the total amount of water retrieved in the river stretch against the recorded hydrometric values for each of the time considered time intervals. The linear regression is depicted in Figure 7, showing R^2 values of 0.8398 and 0.8356 for Spessa Po (a) and Piacenza (b) sections respectively. The high correlation proofs the effectiveness of the methodology in describing the fluctuation of the water quantity in the river stream on the considered reference period.

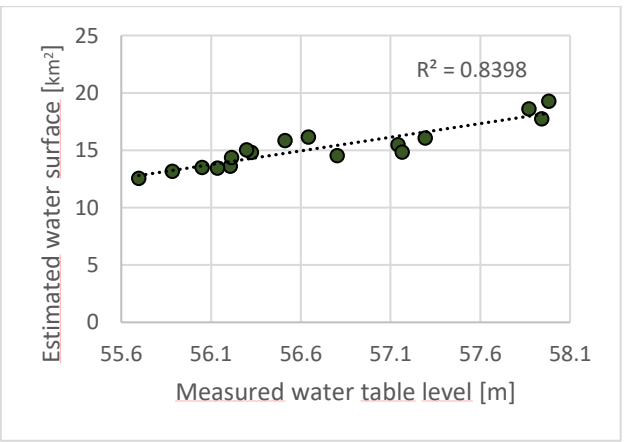

(a)

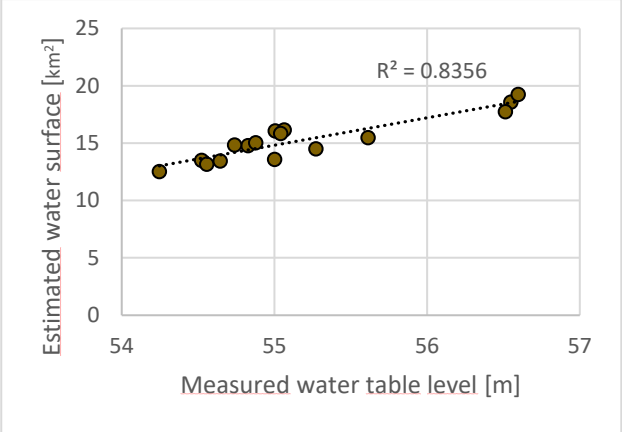

(b)

Figure 7. Correlation between the measured water levels and the estimated water surface in the section of (a) Spessa Po and (b) Piacenza within the whole considered time range (May 2016-2023).

5. CONCLUSIONS

This work proposes a methodology to exploit optical (Sentinel-2) and radar (Sentinel-1) satellite imagery to detect water surface and monitor permanent medium-width rivers. Such a methodology will then be offered to public administration to enlarge the set of available tools of territorial monitoring, so to strengthen the capability of responding to drought events. The data fusion is performed through a Random Forest algorithm run on Google Earth Engine platform. This tool offers a great advantage when dealing with heavy and multitemporal image processing, but it is relevant to remember that it is not an opensource software. In consequence, it is possible to use it freely for academic purposes and exploit its functionalities also for reaching non-proprietary datasets, but it would require a license and/or agreement in case of production of a real application to be actually used by governmental authorities.

The system has been demonstrated to be reliable in classifying water pixels with sufficiently high levels of accuracy for the considered study case, but it is to be remarked that results are strongly related to data quality and to training set used for training the machine learning algorithm. While commonly employed methods of optical or radar image processing, e.g. thresholding methods, may encounter errors due to meteorological conditions or noise in signal, the proposed method is capable of compensating the most typical misclassification and taking advantage of the best information from the two datasets. Anyway, it should be noticed that due to different conditions, e.g. unavailability of optical data for a long time for cloud coverage, some data may be missing requiring to change the reference time window. It is relevant to state that the necessities expressed by the final users (Regione Lombardia in this case) were crucial to shape the work itself. The proposed tool, in facts, aims to provide a practical support for short/medium-term monitoring, thus allowing to be flexible in terms of time window selection for the analyses. Indeed, a near-real time monitoring may not be possible in a system such the proposed one due to possible unavailability of satellite images for the selected dates; nevertheless, it should be pointed out that early warnings systems (e.g. for floods) are already active and based on real time data such as the hydrometric records exploited also during the current work.

In terms of training set, it would be interesting to explore the possibility of automatizing the selection of representative geometries. A partial solution would be the extraction of a base set of polygons deemed as sufficiently representative. Then for each monitoring in subsequent epochs, if necessary, the training polygons could be updated, without the need of re-building the whole set.

As foreseen development, it may be of interest to test different machine learning algorithms for improving results quality, as well as integrating in the system additional parameters to estimate more precisely water volume variations. In this direction, it is reasonable to think about the insertion of 3D flow modelling (in case of sections with known geometries). Furthermore, also data coming from rain gauges and reservoir discharges could be considered as reference datasets for the validation of the methodology.

Lastly, it would be also of interest to explore the different typologies of streams that can actually be monitored through the presented methodology. Rivers characterized by different morphologies may not respond as well as Po; as an example, a stream with a more regular and constant section might not show the same behaviour in terms of water surface and water level correlation, thus resulting in a less accurate mapping of water coverage differences. Nevertheless, it is Regione Lombardia interest to obtain a tool that can be as much as possible flexible, to be used for monitoring diverse rivers, so to support the related policies. All in all, the proposed methodology shows to be promising. The final goal is recognized in a profitable integration of the water mapping procedure in official territorial policies and monitoring plans. In this case, it would be reasonable to provide to public administration also open complementary datasets, such as the drought indices suggested by the World Meteorological Organization (WMO, 2016).

ACKNOWLEDGEMENTS

This work is developed within the *Innovazione* project (2022) by Regione Lombardia in partnership with Politecnico di Milano. The research was triggered and constantly supported by Struttura Natura e Biodiversità, belonging to Regione Lombardia Direzione Territorio e Sistemi Verdi.

The authors wish to thank MSc student Francesco Gioia for his contribution to the development of part of the GEE code.

The maps proposed in the work contain modified Copernicus Sentinel data [2022].

REFERENCES

AIPo, 2022. Avviso alla navigazione 22 giugno 2022. Retrieved June 17 2023 from https://www.agenziapo.it/content/avviso-alla-navigazione.

AIPo, 2023a. English presentation. *Agenzia Interregionale per il Fiume Po*. Retrieved June 17 2023 from https://www.agenziapo.it/content/english-presentation.

AIPo, 2023b. Geoportale. *Agenzia Interregionale per il Fiume Po*. Retrieved June 17 2023 from http://geoportale.agenziapo.it/web/index.php/it/?option=com_aipografd3.

Ajmar, A., Boccardo, P., Broglia, M., Kucera, J., Giulio-Tonolo, F., & Wania, A, 2017: Response to flood events: The role of satellite-based emergency mapping and the experience of the Copernicus emergency management service. In Flood damage

survey and assessment: New insights from research and practice (213–228), *Geophysical Monograph* 228, John Wiley & Sons, Inc., Hoboken, NJ, USA, ISBN: 978-1-119-21792-3. doi:10.1002/9781119217930.ch14.

Autorità di Bacino Distrettuale del Fiume Po, 2022. Bollettino n.17/2022 (12/10/2022). *Osservatorio Permanente sugli utilizzi idrici nel Distretto idrografico del Fiume Po*. https://adbpo.it/osservatorio-permanente/.

Bazi, Y., Bruzzone, L., Melgani, F., 2005: An unsupervised approach based on the generalized Gaussian model to automatic change detection in multitemporal SAR images. *IEEE Transactions on Geoscience and Remote Sensing*, vol. 43, no. 4, pp. 874-887, April 2005. https://doi.org/10.1109/tgrs.2004.842441.

Bonaldo, D., Bellafiore, D., Ferrarin, C., Ferretti, R., Ricchi, A., Sangelantoni, L., Vitelletti, M.L., 2022. The summer 2022 drought: a taste of future climate for the Po valley (Italy)?. *Reg Environ Change* **23**, 1 (2023). https://doi.org/10.1007/s10113-022-02004-z.

Breiman, L., 2001: Random Forests. Machine learning, 45, 5-32. https://doi.org/10.1023/A:1010950718922.

Cao, H., Zhang, H., Wang, C., Zhang, B., 2019: Operational Flood Detection Using Sentinel-1 SAR Data over Large Areas. *Water*. 2019; 11(4):786. https://doi.org/10.3390/w11040786.

Carreño Conde, F. & De Mata Muñoz, M., 2019. Flood Monitoring Based on the Study of Sentinel-1 SAR Images: The Ebro River Case Study. *Water* 2019, 11, 2454. https://doi.org/10.3390/w11122454.

Chakhar, A., Hernández-López, D., Ballesteros, R., Moreno, M.A., 2021. Improving the Accuracy of Multiple Algorithms for Crop Classification by Integrating Sentinel-1 Observations with Sentinel-2 Data. *Remote Sens*. 2021, 13, 243. https://doi.org/10.3390/ rs13020243.

Coldiretti, 2022. Siccità: il Po più in secca che a ferragosto. Articolo. Meteo e clima. Retrieved June 17 2023 from https://www.coldiretti.it/meteo_clima/siccita-il-po-piu-in-secca-che-a-ferragosto#:~:text=L%E2%80%99assenza%20di%20precipitazioni%20che%20in%20certe%20zone%20ha,duro%20per%20la%20pasta%20e%20il%2073%25%20dell%E2%80%99orzo.

D'Amato, A., 2022. Stop all'acqua anche di giorno: i piani per il razionamento nelle regioni e lo stato d'emergenza in arrivo. *OPEN*. Retrieved June 17 2023 from https://www.open.online/2022/06/28/siccita-razionamento-acqua-regioni-stop-giorno/.

De Fioravante, P., Luti, T., Cavalli, A., Giuliani, C., Dichicco, P., Marchetti, M., Chirici, G., Congedo, L., Munafò, M., 2021. Multispectral Sentinel-2 and SAR Sentinel-1 Integration for Automatic Land Cover Classification. *Land* 2021, 10, 611. https://doi.org/10.3390/land10060611.

ESA, 2023a. Sentinel-2 mission guide. Retrieved June 17 2023 from https://sentinel.esa.int/web/sentinel/missions/sentinel-2.

ESA, 2023b. Mission summary. Sentinel-1. Retrieved June 17 2023 from https://sentinels.copernicus.eu/web/sentinel/missions/sentinel-1/overview/mission-summary.

Felegari, S., Sharifi, A., Moravej, K., Amin, M., Golchin, A., Muzirafuti, A., Tariq, A., Zhao, N., 2021. Integration of Sentinel 1 and Sentinel 2 Satellite Images for Crop Mapping. *Appl. Sci*. 2021, 11, 10104. https://doi.org/10.3390/ app112110104.

Gascon, F., Bouzinac, C., Thépaut, O., Jung, M., Francesconi, B., Louis, J., Lonjou, V., Lafrance, B., Massera, S., Gaudel-Vacaresse, A., Languille, F., Alhammoud, B., Viallefont, F., Pflug, B., Bieniarz, J., Clercl, S., Pessiot, L., Trémas, T., Cadau, E., De Bonis, R., Isola, C., Martimort, P., Fernandez, V., 2017. Copernicus Sentinel-2A Calibration and Products Validation Status. *Remote Sens.* 2017, *9*, 584. https://doi.org/10.3390/rs9060584.

GDO, 2023. Global Drought Observatory. Emergency Management Service. *Copernicus*. European Commission. Retrieved June 17 2023 from https://edo.jrc.ec.europa.eu/gdo.

GEE, 2023. Sentinel Collections. *Earth Engine Data Catalog*. Retrieved June 2017 2023 from https://developers.google.com/earth-engine/datasets/catalog/sentinel.

Gorelick, N., Hancher, M., Dixon, M., Ilyushchenko, S., Thau, D., Moore, R., 2017. Google Earth Engine: Planetary-scale geospatial analysis for everyone. *Remote SensingRemote Sensing of Environment.*
Gustafsson, F., 2012. Statistical Sensor Fusion, 2nd ed. Lund, Germany: Studentlitteratur.

JRC, 2011. NDWI: Normalized Difference Water Index. Product fact sheet: NDWI – Europe. DESERT Action – LMNH Unit. European Commission.

Landuyt, L.,Van Wesemael, A., Schumann, G.J.P., Hostache, R., Verhoest, N.E.C., Van Coillie, F.M.B., 2019. Flood Mapping Based on Synthetic Aperture Radar: An Assessment of Established Approaches. *IEEE Transactions on Geoscience and Remote SensingRemote Sensing*, vol. 57, no. 2, pp. 722-739, Feb. 2019. https://doi.org/10.1109/tgrs.2018.2860054.

Langat, P. K., Kumar, L., Koech, R., 2019: Monitoring river channel dynamics using remote sensingRemote Sensing and GIS techniques. Geomorphology. Volume 325. Pages 92-102. ISSN 0169-555X. https://doi.org/10.1016/j.geomorph.2018.10.007.

Levantesi, S., 2017: Italy must prepare for a future of chronic drought. *Nature Italy – Q&A*. https://doi.org/10.1038/d43978-022-00089-y.

Li, M., Zhang, T., Tu, Y., Ren, Z., Xu, B., 2022. Monitoring Post-Flood Recovery of Croplands Using the Integrated Sentinel-1/2 Imagery in the Yangtze-Huai River Basin. *Remote Sens*. 2022, 14, 690. https://doi.org/ 10.3390/rs14030690.

Milczarek M., Robak, A., Gadawska, A., 2017: Sentinel Water Mask (SWM) – New index for water detection on Sentinel-2 images. 7th Advanced Training Course on Land Remote SensingRemote Sensing, Szent István University, Gödöllő, Hungary.

Povoledo, E., 2023. Flood-Battered Italian Region May See More Violent and Frequent Storms. *The New York Times*. Retrieved June 17 2023 from

https://www.nytimes.com/2023/05/27/world/europe/italy-floods-emilia-romagna.html.

Ramadhani, F., Pullanagari, R., Kereszturi, G., Procter, J., 2020. Automatic Mapping of Rice Growth Stages Using the Integration of SENTINEL-2, MOD13Q1, and SENTINEL-1. *Remote Sens*. 2020, 12, 3613. https://doi.org/10.3390/rs12213613.

Regione Lombardia, 2022: Deliberazione della giunta regionale 13 aprile 2022, n. XI/6283, Dichiarazione dello stato di severità idrica media in Regione Lombardia e determinazioni conseguenti – disposizioni in materia di deroghe temporanee al rilascio del deflusso minimo vitale/deflusso ecologico.

Schmitt, M. & Zhu, X.X., 2016. Data Fusion and Remote SensingRemote Sensing: An ever-growing relationship. *IEEE Geoscience and Remote SensingRemote Sensing Magazine*, vol. 4, no. 4, pp. 6-23, Dec. 2016, https://doi.org/10.1109/mgrs.2016.2561021.

Ting, K.M., 2011: Confusion Matrix. In: Sammut, C., Webb, G.I. (eds) Encyclopedia of Machine Learning. Springer, Boston, MA. https://doi.org/10.1007/978-0-387-30164-8_157.

Tomsett, C., & Leyland, J., 2019. Remote sensingRemote Sensing of river corridors: A review of current trends and future directions. *River Res. Appl*. 35 (7), 779–803. doi:10.1002/rra.3479.

Toreti, A., Bavera, D., Avanzi, F., Cammalleri, C., De Felice, M., de Jager, A., Di Ciollo, C., Gabellani, S., Maetens, W., Magni, D., Manfron G., Masante, D., Mazzeschi, M., McCormick, N., Naumann, G., Niemeyer, S., Rossi, L., Seguini, L., Spinoni, J., van den Berg, M., Drought in northern Italy March 2022, EUR 31037 EN, Publications Office of the European Union, Luxembourg, 2022, ISBN 978-92-76-50158-9 (online), doi:10.2760/781876 (online), JRC128974.

Tuvdendorj, B., Zeng, H., Wu, B., Elnashar, A., Zhang, M., Tian, F., Nabil, M., Nanzad, L., Bulkhbai, A., Natsagdorj, N., 2022. Performance and the Optimal Integration of Sentinel-1/2 Time-Series Features for Crop Classification in Northern Mongolia. *Remote Sens*. 2022, 14, 1830. https://doi.org/10.3390/rs14081830.

Twele, A., Cao, W., Plank, S., Martinis, S., 2016. Sentinel-1-based flood mapping: a fully automated processing chain. *International Journal of Remote SensingRemote Sensing*, 37:13, 2990-3004. https://doi.org/10.1080/01431161.2016.1192304.

Vavassori, A., Carrion, D., Zaragozi, B., Migliaccio, F., 2022: VGI and Satellite Imagery Integration for Crisis Mapping of Flood Events. *ISPRS Int. J. Geo-Inf. 2022*, 11, 611. https://doi.org/10.3390/ijgi11120611.

World Meteorological Organization (WMO) and Global Water Partnership (GWP), 2016: Handbook of Drought Indicators and Indices. (M. Svoboda and B.A. Fuchs). Integrated Drought Management Programme (IDMP), *Integrated Drought Management Tools and Guidelines Series 2*. Geneva. ISBN 978-92-63-11173-9.